

Safe Policy Learning for Continuous Control

Yinlam Chow

Google Research

yinlamchow@google.com

Ofir Nachum

Google Research

ofirnachum@google.com

Aleksandra Faust

Google Research

sandrafaust@google.com

Edgar Dueñez-Guzman

DeepMind

duenez@google.com

Mohammad Ghavamzadeh

Google Research

ghavamza@google.com

Keywords: constrained MDPs, reinforcement learning, safety, robot navigation

Abstract: We study continuous action reinforcement learning problems in which it is crucial that the agent interacts with the environment only through *near-safe* policies, i.e., policies that keep the agent in desirable situations, both during training and at convergence. We formulate these problems as *constrained* Markov decision processes (CMDPs) and present safe policy optimization algorithms that are based on a *Lyapunov* approach to solve them. Our algorithms can use any standard policy gradient (PG) method, such as deep deterministic policy gradient (DDPG) or proximal policy optimization (PPO), to train a neural network policy, while enforcing near-constraint satisfaction for every policy update by projecting either the policy parameter or the selected action onto the set of feasible solutions induced by the state-dependent linearized Lyapunov constraints. Compared to the existing constrained PG algorithms, ours are more data efficient as they are able to utilize both on-policy and off-policy data. Moreover, in practice our action-projection algorithm often leads to less conservative policy updates and allows for natural integration into an end-to-end PG training pipeline. We evaluate our algorithms and compare them with the state-of-the-art baselines on several simulated (MuJoCo) tasks, as well as a real-world robot obstacle-avoidance problem, demonstrating their effectiveness in terms of balancing performance and constraint satisfaction.

1 Introduction

The field of reinforcement learning (RL) has witnessed tremendous success in many high-dimensional control problems, including video games [1], board games [2], robot locomotion [3], manipulation [4, 5], navigation [6], and obstacle avoidance [7]. In RL, the ultimate goal is to optimize the expected sum of rewards/costs, and the agent is free to explore any behavior as long as it leads to performance improvement. Although this freedom might be acceptable in problems that have access to a simulator, it might be harmful in many other problems and could damage the agent (robot) or the environment (objects or people nearby). In such domains, it is absolutely crucial that while the agent optimizes its long-term performance, it only executes safe policies both during training and at convergence.

A natural way to incorporate safety is via constraints. A standard model for RL with constraints is constrained Markov decision process (CMDP) [8], where in addition to its standard objective, the agent must satisfy constraints on the expectation of some auxiliary costs. Although optimal policies for finite CMDPs with known models can be obtained by linear programming [8], there are not many results for solving CMDPs when the model is unknown or the state and/or action spaces are large or infinite. A common approach to solve CMDPs is to use the Lagrangian method [9, 10], which augments the original objective function with a penalty on constraint violation and computes the saddle-point of the constrained policy optimization via primal-dual methods [11]. Although safety is ensured for the generated policy upon convergence, a major drawback of this approach is that it makes no guarantee with regards to the safety of the policies generated during training.

A few algorithms have been recently proposed to solve CMDPs at scale while remaining safe during training. One such algorithm is *constrained policy optimization* (CPO) [12, 13]. CPO extends the trust-region policy optimization (TRPO) algorithm [14] to handle the constraints in a principled way and has shown promising empirical results in terms scalability, performance, and constraint

satisfaction, both during training and at convergence. Another class of these algorithms is by Chow et al. [15]. These algorithms use the notion of Lyapunov function that has a long history in control theory to analyze the stability of dynamical systems [16]. Lyapunov functions have been used in RL to guarantee closed-loop stability [17, 18]. They also have been used to guarantee that a model-based RL agent can be brought back to a “region of attraction” during exploration [19]. Chow et al. [15] use the properties of the Lyapunov functions and propose approximate policy and value iteration algorithms that generate safe policies during training and at convergence. They prove theories for their algorithms when the CMDP is finite with known dynamics, and empirically evaluate them when the state space is large (or infinite) and the CMDP model is unknown. However, their algorithms are value-function-based, and thus, are restricted to discrete-action problems.

In this paper, we extend the Lyapunov-based approach of Chow et al. [15] to problems with large or infinite action spaces, and propose safe RL algorithms for these problems that return safe policies both during training and at convergence. For this extension, we need to address two major issues: **1)** the policy update requires solving an optimization problem over the large or continuous action space, and **2)** the objective function and (Lyapunov) constraint of this problem involve integration over the action space, which can be numerically intractable. Since the number of Lyapunov constraints is equal to the number of states, the situation is even more challenging when the problem has a large state space. To address the first difficulty, we focus on policy gradient (PG) algorithms. To address the second difficulty, we propose two approaches to solve our constrained policy optimization problem (a problem with infinite constraints, each involving an integral over the continuous action space) that can work with any standard on-policy (e.g., proximal policy optimization (PPO) [20]) and off-policy (e.g., deep deterministic policy gradient (DDPG) [3]) PG algorithm. Our first approach, which we call *policy parameter projection* or *θ -projection*, is a constrained optimization method that combines PG with a projection of the policy parameters onto the set of feasible solutions induced by the Lyapunov constraints. Our second approach, which we call *action projection* or *a -projection*, utilizes the *safety layer* concept [21] with Lyapunov functions to derive a closed-form approximate solution of the constrained policy optimization problem and integrates that into the policy network. Since both approaches guarantee safety at every policy update, they manage to enforce safety throughout training (in the absence of function approximation error), ensuring all intermediate policies are safe to be deployed. To prevent constraint violation due to function approximation error, similar to CPO, we offer a safeguard policy update rule that further decreases the constraint cost.

Our proposed algorithms have two main advantages over CPO. First, since CPO is closely connected to TRPO, it can be only trivially combined with on-policy PG algorithms, such as PPO. On the contrary, our algorithms can work with any on-policy (e.g., PPO) and off-policy (e.g., DDPG) PG algorithm. Having an off-policy implementation has the potential benefit of being more data-efficient, since it allows using data from the replay buffer. Second, while CPO is not a *back-propagatable* algorithm, due to the backtracking line-search procedure and the conjugate gradient iterations for computing natural gradient in TRPO, our *a -projection* algorithm can be trained *end-to-end*, which is crucial for scalable and efficient implementation [22]. More importantly, we show in Section 3.1 that CPO (minus the line search) can be viewed as a special case of the on-policy version (PPO version) of our θ -projection algorithm, corresponding to a specific approximation of the constraints.

We empirically evaluate our algorithms and compare them with CPO and the Lagrangian method on several continuous control (MuJoCo) tasks and a real-world robot navigation problem, in which the robot must satisfy certain constraints, while minimizing its expected cumulative cost. Results show that our algorithms outperform the baselines in terms of balancing performance and near-constraint satisfaction (during training), and generalize better to unseen environments.

2 Preliminaries

We consider the RL problem in which the agent’s interaction with the environment is modeled as a Markov decision process (MDP). A MDP is a tuple $(\mathcal{X}, \mathcal{A}, \gamma, c, P, x_0)$, where \mathcal{X} and \mathcal{A} are the state and action spaces; $\gamma \in [0, 1]$ is a discounting factor; $c(x, a) \in [0, C_{\max}]$ is the immediate cost function; $P(\cdot|x, a)$ is the transition probability distribution; and $x_0 \in \mathcal{X}$ is the initial state. Although we consider deterministic initial state and cost function, our results can be easily generalized to random initial states and costs. We model the RL problems in which there are constraints on the cumulative cost using CMDPs. The CMDP model extends MDP by introducing two additional components: the state-dependent constraint cost $d(x) \in [0, D_{\max}]$ and the constraint cost threshold $d_0 \in \mathbb{R}_{\geq 0}$.

We now formalize the CMDP optimization problem. Let Δ be the set of Markovian stationary policies, i.e., $\Delta = \{\pi : \mathcal{X} \times \mathcal{A} \rightarrow [0, 1], \sum_a \pi(a|x) = 1\}$. At each state $x \in \mathcal{X}$, we define the generic Bellman operator w.r.t. a policy $\pi \in \Delta$ and a cost function h as $T_{\pi, h}[V](x) = \sum_{a \in \mathcal{A}} \pi(a|x) [h(x, a) +$

$\gamma \sum_{x' \in \mathcal{X}} P(x'|x, a) V(x')$. Given a policy $\pi \in \Delta$, we define the expected cumulative cost as $\mathcal{C}_\pi(x_0) := \mathbb{E}[\sum_{t=0}^{\infty} \gamma^t c(x_t, a_t) \mid \pi, x_0]$ and the safety constraint function (i.e., expected cumulative constraint cost) as $\mathcal{D}_\pi(x_0) := \mathbb{E}[\sum_{t=0}^{\infty} \gamma^t d(x_t) \mid \pi, x_0]$. The *safety constraint*¹ is then defined as $\mathcal{D}_\pi(x_0) \leq d_0$. The goal in CMDPs is to solve the constrained optimization problem

$$\pi^* \in \arg \min_{\pi \in \Delta} \{ \mathcal{C}_\pi(x_0) : \mathcal{D}_\pi(x_0) \leq d_0 \}. \quad (1)$$

It has been shown that if the feasibility set is non-empty, then there exists an optimal policy in the class of stationary Markovian policies Δ [8, Theorem 3.1].

2.1 Lyapunov Functions

Since our algorithms are developed within the Lyapunov-based formulation of Chow et al. [15], we end this section by introducing the terminology of this setting. We refer the readers to Appendix B for more details. We define a set of Lyapunov functions w.r.t. initial state $x_0 \in \mathcal{X}$ and constraint threshold d_0 as $\mathcal{L}_{\pi_B}(x_0, d_0) = \{L : \mathcal{X} \rightarrow \mathbb{R}_{\geq 0} \mid T_{\pi_B, d}[L](x) \leq L(x), \forall x \in \mathcal{X}, L(x_0) \leq d_0\}$, where π_B is a feasible policy of (1), i.e., $\mathcal{D}_{\pi_B}(x_0) \leq d_0$. We refer to the constraints in this set as the *Lyapunov constraints*. For an arbitrary Lyapunov function $L \in \mathcal{L}_{\pi_B}(x_0, d_0)$, we denote by $\mathcal{F}_L = \{\pi \in \Delta : T_{\pi, d}[L](x) \leq L(x), \forall x \in \mathcal{X}\}$, the set of L -induced stationary policies. The contraction property of $T_{\pi, d}$, together with $L(x_0) \leq d_0$, imply that any L -induced policy in \mathcal{F}_L is a feasible policy of (1). However, $\mathcal{F}_L(x)$ does not always contain an optimal solution of (1), and thus, it is necessary to design a Lyapunov function that provides this guarantee. In other words, the main goal of the Lyapunov approach is to construct a Lyapunov function $L \in \mathcal{L}_{\pi_B}(x_0, d_0)$, such that \mathcal{F}_L contains an optimal policy π^* , i.e., $L(x) \geq T_{\pi^*, d}[L](x)$. Theorem 1 in [15] shows that without loss of optimality, the Lyapunov function that satisfies the above criterion can be expressed as $L_{\pi_B, \epsilon}(x) := \mathbb{E}[\sum_{t=0}^{\infty} \gamma^t (d(x_t) + \epsilon(x_t)) \mid \pi_B, x]$, where $\epsilon(x) \geq 0$ is a specific immediate *auxiliary constraint cost* that keeps track of the maximum *constraint budget* available for policy improvement (from π_B to π^*). However, computing ϵ is challenging for general problems. Therefore, in our work we replace that with a constraint cost surrogate $\tilde{\epsilon}$, which is a tight upper-bound on ϵ and can be computed more efficiently (see Appendix B). Utilizing this approximation, we may write the safe policy optimization problem as the following linear program (LP):

$$\pi_+(\cdot|x) = \arg \min_{\pi \in \Delta} \int_{a \in \mathcal{A}} Q_{V_{\pi_B}}(x, a) \pi(a|x) \quad \text{s.t.} \quad \int_{a \in \mathcal{A}} Q_{L_{\pi_B}}(x, a) (\pi(a|x) - \pi_B(a|x)) \leq \tilde{\epsilon}(x), \quad (2)$$

where $V_{\pi_B}(x) = T_{\pi_B, c}[V_{\pi_B}](x)$ and $Q_{V_{\pi_B}}(x, a) = c(x, a) + \gamma \sum_{x'} P(x'|x, a) V_{\pi_B}(x')$ are the value and state-action value functions (w.r.t. the cost function c), and $Q_{L_{\pi_B}}(x, a) = d(x) + \tilde{\epsilon}(x) + \gamma \sum_{x'} P(x'|x, a) L_{\pi_B, \tilde{\epsilon}}(x')$ is the Lyapunov function. In any iterative policy optimization method, such as those we study in this paper, the feasible baseline policy π_B at each iteration can be set to the policy computed at the previous iteration (which is feasible). The LP in (2) can be numerically intractable as the constraint involves an integral over the entire action space. This was not an issue for Chow et al. [15], because they only studied problems with finite number of actions. However, this is problematic for us, since our focus is on continuous action problems. In the next section, we use PG and propose two methods to (approximately) solve (2).

3 Safe Lyapunov-based Policy Gradient

Policy gradient (PG) algorithms optimize a policy by computing a sample estimate of the gradient of the expected cumulative cost induced by the policy, and then updating the policy parameter in the gradient direction. In general, stochastic policies that give a probability distribution over actions are parameterized by a κ -dimensional vector θ , so the space of policies can be written as $\{\pi_\theta, \theta \in \Theta \subset \mathbb{R}^\kappa\}$. Since in this setting a policy π is uniquely defined by its parameter θ , policy-dependent functions can be written as a function of θ or π interchangeably.

To guarantees safety (both at convergence and during training) in our proposed Lyapunov-based algorithms, we need to extend PG to solve CMDPs, and in particular to solve the constrained optimization problem (2). Our algorithms consist of two main components, a baseline PG algorithm, such as DDPG or PPO, and an effective method to solve the following Lyapunov-based policy optimization problem that is analogous to (2):

$$\theta_+ = \arg \min_{\theta \in \Theta} \mathcal{C}_{\pi_\theta}(x_0), \quad \text{s.t.} \quad \int_{a \in \mathcal{A}} (\pi_\theta - \pi_B)(a|x) Q_{L_{\pi_B}}(x, a) da \leq \tilde{\epsilon}(x), \quad \forall x \in \mathcal{X}. \quad (3)$$

¹The notion of safety in this work is modeled by the CMDP constraint, which is different from that considered in control theory in which safety is based on satisfaction of hard constraints.

In the next two sections, we present two approaches to solve (3) efficiently. We call these approaches **1)** θ -projection, a constrained optimization method that combines PG with projection of the policy parameter θ onto the set of feasible solutions induced by the Lyapunov constraints, and **2)** a -projection, in which we embed the Lyapunov constraints into the policy network via a safety layer.

3.1 The θ -projection Approach

The θ -projection approach is based on the *minorization-maximization* technique in conservative PG [23] and Taylor series expansion, and can be applied to both on-policy and off-policy algorithms. Following Theorem 4.1 in Kakade and Langford [23], we first have the following bound for the cumulative cost: $-\beta\overline{D}_{\text{KL}}(\theta, \theta_B) \leq \mathcal{C}_{\pi_\theta}(x_0) - \mathcal{C}_{\pi_{\theta_B}}(x_0) - \mathbb{E}_{x \sim \mu_{\theta_B}, x_0, a \sim \pi_\theta} [Q_{V_{\theta_B}}(x, a) - V_{\theta_B}(x)] \leq \beta\overline{D}_{\text{KL}}(\theta, \theta_B)$, where μ_{θ_B, x_0} is the γ -visiting distribution of π_{θ_B} starting at the initial state x_0 , $\overline{D}_{\text{KL}}(\theta, \theta_B) = \mathbb{E}_x [D_{\text{KL}}(\pi_\theta(\cdot|x) || \pi_{\theta_B}(\cdot|x))]$ is the average relative entropy, and β is the weight for the entropy regularization.² Using this result, we denote by $\mathcal{C}'_{\pi_\theta}(x_0; \pi_{\theta_B}) = \mathcal{C}_{\pi_{\theta_B}}(x_0) + \beta\overline{D}_{\text{KL}}(\theta, \theta_B) + \mathbb{E}_{x \sim \mu_{\theta_B}, x_0, a \sim \pi_\theta} [Q_{V_{\theta_B}}(x, a) - V_{\theta_B}(x)]$, the surrogate cumulative cost. It has been shown in Eq. 10 of [14] that replacing the objective function $\mathcal{C}_{\pi_\theta}(x_0)$ with its surrogate $\mathcal{C}'_{\pi_\theta}(x_0; \pi_{\theta_B})$ in solving (3) will still lead to policy improvement. In order to effectively compute the improved policy parameter θ_+ , one further approximates the function $\mathcal{C}'_{\pi_\theta}(x_0; \pi_{\theta_B})$ with its Taylor series expansion around θ_B . In particular, the term $\mathbb{E}_{x \sim \mu_{\theta_B}, x_0, a \sim \pi_\theta} [Q_{V_{\theta_B}}(x, a) - V_{\theta_B}(x)]$ is approximated up to its first order, and the term $\overline{D}_{\text{KL}}(\theta, \theta_B)$ is approximated up to its second order. These altogether allow us to replace the objective function in (3) with $\langle (\theta - \theta_B), \nabla_\theta \mathbb{E}_{x \sim \mu_{\theta_B}, x_0, a \sim \pi_\theta} [Q_{V_{\theta_B}}(x, a)] \rangle + \frac{\beta}{2} \langle (\theta - \theta_B), \nabla_\theta^2 \overline{D}_{\text{KL}}(\theta, \theta_B) |_{\theta=\theta_B} (\theta - \theta_B) \rangle$. Similarly, regarding the constraints in (3), we can use the Taylor series expansion (around θ_B) to approximate the LHS of the Lyapunov constraints as $\int_{a \in \mathcal{A}} (\pi_\theta - \pi_B)(a|x) Q_L(x, a) da \approx \langle (\theta - \theta_B), \nabla_\theta \mathbb{E}_{a \sim \pi_\theta} [Q_{L_{\theta_B}}(x, a)] |_{\theta=\theta_B} \rangle$. Using the above approximations, at each iteration, our safe PG algorithm updates the policy by solving the following constrained optimization problem with *semi-infinite dimensional* Lyapunov constraints:

$$\begin{aligned} \theta_+ \in \arg \min_{\theta \in \Theta} & \langle (\theta - \theta_B), \nabla_\theta \mathbb{E}_{x \sim \mu_{\theta_B}, x_0, a \sim \pi_\theta} [Q_{V_{\theta_B}}(x, a)] \rangle + \frac{\beta}{2} \langle (\theta - \theta_B), \nabla_\theta^2 \overline{D}_{\text{KL}}(\theta, \theta_B) |_{\theta=\theta_B} (\theta - \theta_B) \rangle, \\ \text{s.t. } & \langle (\theta - \theta_B), \nabla_\theta \mathbb{E}_{a \sim \pi_\theta} [Q_{L_{\theta_B}}(x, a)] |_{\theta=\theta_B} \rangle \leq \tilde{\epsilon}(x), \forall x \in \mathcal{X}. \end{aligned} \quad (4)$$

It can be seen that if the errors resulted from the neural network parameterizations of $Q_{V_{\theta_B}}$ and $Q_{L_{\theta_B}}$, and the Taylor series expansions are small, then an algorithm that updates the policy parameter by solving (4) can ensure safety during training. However, the presence of infinite-dimensional Lyapunov constraints makes solving (4) intractable. A solution to this is to write the Lyapunov constraints in (4) (without loss of optimality) as $\max_{x \in \mathcal{X}} \langle (\theta - \theta_B), \nabla_\theta \mathbb{E}_{a \sim \pi_\theta} [Q_{L_{\theta_B}}(x, a)] |_{\theta=\theta_B} \rangle - \tilde{\epsilon}(x) \leq 0$. Since the above max-operator is non-differentiable, this may still lead to numerical instability in gradient descent algorithms. Similar to the surrogate constraint in TRPO (to transform the max D_{KL} constraint to an average \overline{D}_{KL} constraint, see Eq. 12 in Schulman et al. [14]), a more numerically stable solution is to *approximate* the Lyapunov constraint using the average constraint surrogate as

$$\langle (\theta - \theta_B), \frac{1}{M} \sum_{i=1}^M \nabla_\theta \mathbb{E}_{a \sim \pi_\theta} [Q_{L_{\theta_B}}(x_i, a)] |_{\theta=\theta_B} \rangle \leq \frac{1}{M} \sum_{i=1}^M \tilde{\epsilon}(x_i), \quad (5)$$

where M is the number of on-policy sample trajectories of π_{θ_B} . In order to effectively compute the gradient of the Lyapunov value function, consider the special case when the auxiliary constraint surrogate is chosen as $\tilde{\epsilon} = (1 - \gamma)(d_0 - \mathcal{D}_{\pi_{\theta_B}}(x_0))$ (see Appendix B for justification). Using the fact that $\tilde{\epsilon}$ is θ -independent, the gradient term in (5) can be written as $\int_a \pi_\theta(a|x) \nabla_\theta \log \pi_\theta(a|x) Q_{W_{\theta_B}}(x, a) da$, where $W_{\theta_B}(x) = T_{\pi_B, d}[W_{\theta_B}](x)$ and $Q_{W_{\theta_B}}(x, a) = d(x) + \gamma \sum_{a'} P(a'|x, a) W_{\theta_B}(a')$ are the constraint value and action-value functions, respectively. Since the integral in the gradient term is equal to $E_{a \sim \pi_\theta} [Q_{W_{\theta_B}}(x, a)]$, the average constraint surrogate (5) can be approximated (because of the choice of $\tilde{\epsilon}$) by the inequality $\mathcal{D}_{\pi_{\theta_B}}(x_0) + \langle \frac{(\theta - \theta_B)}{1 - \gamma}, \frac{1}{M} \sum_{i=1}^M \nabla_\theta \mathbb{E}_{a \sim \pi_\theta} [Q_{W_{\theta_B}}(x_i, a)] |_{\theta=\theta_B} \rangle \leq d_0$, which is equivalent to the constraint used in CPO (see Section 6.1 in [12]). This shows that CPO (minus the line search) belongs to the class of our Lyapunov-based PG algorithms with θ -projection. We refer to the DDPG and PPO versions of our θ -projection safe PG algorithms as SDDPG and SPPO. Derivation details and the pseudo-code (Algorithm 4) of these algorithms are given in Appendix C.

²Theorem 1 in Schulman et al. [14] provides a recipe for computing β such that the minorization-maximization inequality holds, but in practice, β is treated as a tunable parameter for entropy regularization.

3.2 The a -projection Approach

The main characteristic of the Lyapunov approach is to break down a trajectory-based constraint into a sequence of single-step *state dependent* constraints. However, when the state space is infinite, the feasibility set is characterized by infinite dimensional constraints, and thus, it is counter-intuitive to directly enforce the Lyapunov constraints (as opposed to the original trajectory-based constraint) into the policy update optimization. To address this, we leverage the idea of a *safety layer* (defined below by Eq. 6) and propose a novel approach to embed the set of Lyapunov constraints into the policy network. This way, we reformulate the CMDP problem (1) as an unconstrained optimization problem and optimize its policy parameter θ (of the augmented network) using any standard unconstrained PG algorithm. At every given state, the unconstrained action is first computed and then passed through the safety layer, where a feasible action mapping is constructed by projecting unconstrained actions onto the feasibility set w.r.t. Lyapunov constraints. This *constraint projection approach* can guarantee safety during training.

We now describe how the action mapping to the set of Lyapunov constraints works for the case with deterministic policies.³ Recall from the policy improvement problem in (3) that the Lyapunov constraint is imposed at every state $x \in \mathcal{X}$. Given a baseline feasible policy $\pi_B = \pi_{\theta_B}$, for any policy parameter $\theta \in \Theta$, we denote by $\Xi(\pi_B, \theta) = \{\theta' \in \Theta : Q_{L_{\pi_B}}(x, \pi_{\theta'}(x)) - Q_{L_{\pi_B}}(x, \pi_B(x)) \leq \tilde{\epsilon}(x), \forall x \in \mathcal{X}\}$, the *projection* of θ onto the feasibility set induced by the Lyapunov constraints. One way to construct a feasible policy $\pi_{\Xi(\pi_B, \theta)}$ from θ is to solve the following ℓ_2 -projection problem:

$$\pi_{\Xi(\pi_B, \theta)}(x) \in \arg \min_{a \in \mathcal{A}} \frac{1}{2} \|a - \pi_\theta(x)\|^2 \text{ s.t. } Q_{L_{\pi_B}}(x, a) - Q_{L_{\pi_B}}(x, \pi_B(x)) \leq \tilde{\epsilon}(x). \quad (6)$$

We refer to this operation as the *Lyapunov safety layer*. Intuitively, this projection perturbs the unconstrained action as little as possible in the Euclidean norm in order to satisfy the Lyapunov constraints. Since this projection guarantees safety, if we have access to a closed-form of the projection, we may insert it into the policy parameterization and simply solve an unconstrained policy optimization problem, i.e., $\theta_+ \in \arg \min_{\theta \in \Theta} \mathcal{C}_{\pi_{\Xi(\pi_B, \theta)}}(x_0)$, using any standard PG algorithm.

To simplify the projection (6), we can approximate the LHS of the Lyapunov constraint with its first-order Taylor series w.r.t. action $a = \pi_B(x)$. Thus, at any given state $x \in \mathcal{X}$, the safety layer solves the following projection problem:

$$\pi_{\Xi(\pi_B, \theta)}(x) \in \arg \min_{a \in \mathcal{A}} \frac{1-\eta(x)}{2} \|a - \pi_\theta(x)\|^2 + \frac{\eta(x)}{2} \|a - \pi_B(x)\|^2, \text{ s.t. } (a - \pi_B(x))^\top g_{L_{\pi_B}}(x) \leq \tilde{\epsilon}(x), \quad (7)$$

where $\eta(x) \in [0, 1]$ is the mixing parameter that controls the trade-off between projecting on unconstrained policy (for return maximization) and on baseline policy (for safety), and $g_{L_{\pi_B}}(x) := \nabla_a Q_{L_{\pi_B}}(x, a)|_{a=\pi_B(x)}$ is the action-gradient of the state-action Lyapunov function.

Similar to the analysis of Section 3.1, if the auxiliary cost $\tilde{\epsilon}$ is state-independent, one can readily find $g_{L_{\pi_B}}(x)$ by computing the gradient of the constraint action-value function $\nabla_a Q_{W_{\theta_B}}(x, a)|_{a=\pi_B(x)}$. Note that the objective function in (7) is positive-definite and quadratic, and the constraint approximation is linear. Therefore, the solution of this (convex) projection problem can be effectively computed by an in-graph QP-solver, such as OPT-Net [24]. Combined with the above projection procedure, this further implies that the CMDP problem can be effectively solved using an *end-to-end* PG training pipeline (such as DDPG or PPO). When the CMDP has a single constraint (and thus a single Lyapunov constraint), the policy $\pi_{\Xi(\pi_B, \theta)}(x)$ has the following analytical solution.

Proposition 1. *At any given state $x \in \mathcal{X}$, the solution to the optimization problem (7) has the form $\pi_{\Xi(\pi_B, \theta)}(x) = (1-\eta(x))\pi_\theta(x) + \eta(x)\pi_B(x) - \lambda^*(x) \cdot g_{L_{\pi_B}}(x)$, where*

$$\lambda^*(x) = \left[\frac{((1-\eta(x)) \cdot g_{L_{\pi_B}}(x)^\top (\pi_\theta(x) - \pi_B(x)) - \tilde{\epsilon}(x))}{g_{L_{\pi_B}}(x)^\top g_{L_{\pi_B}}(x)} \right]_+.$$

The closed-form solution is essentially a linear projection of the unconstrained action $\pi_\theta(x)$ onto the Lyapunov-safe hyper-plane with slope $g_{L_{\pi_B}}(x)$ and intercept $\tilde{\epsilon}(x) = (1-\gamma)(d_0 - \mathcal{D}_{\pi_B}(x_0))$. We refer to the DDPG and PPO versions of our a -projection safe Lyapunov-based PG algorithms as SDDPG- a and SPPO- a . We report the derivation details and the pseudo-code (Algorithm 5) of these algorithms in Appendix C.

³In our experiments, we use stochastic (Gaussian) policies with parameterized mean and fixed variance. We leave extension of the a -projection approach to policies in which variance is also parameterized as future work.

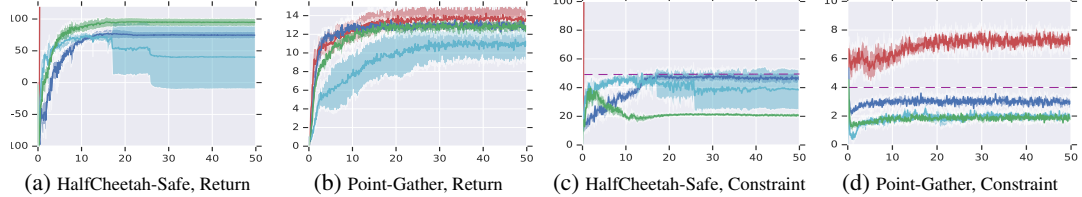


Figure 1: DDPG (red), DDPG-Lagrangian (cyan), SDDPG (blue), SDDPG-a (green) on HalfCheetah-Safe and Point-Gather. SDDPG and SDDPG-a perform stable and are safe during training. Unit of x -axis is in thousand of episodes. Shaded areas represent the 1-SD confidence intervals (over 10 random seeds). The dashed purple line in the figures (c) and (d) represents the constraint limit.

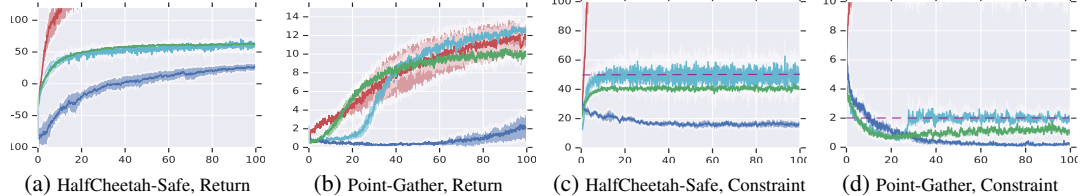


Figure 2: PPO (red), PPO-Lagrangian (cyan), SPPO (blue), SPPO-a (green) on HalfCheetah-Safe and Point-Gather. SPPO-a perform stable and are safe during training. Unit of x -axis is in thousand of episodes. Shaded areas represent the 1-SD confidence intervals (over 10 random seeds). The dashed purple line in the figures (c) and (d) represents the constraint limit.

4 Experiments on MuJoCo Benchmarks

We empirically evaluate our Lyapunov-based safe PG algorithms to assess their performance in terms of: (i) optimizing cost, and (ii) being robust to constraint violation during training. We use three simulated robot locomotion continuous control tasks in the MuJoCo simulator [25].⁴ The notion of safety in these tasks is motivated by physical constraints: (i) HalfCheetah-Safe: this is a modification of the MuJoCo HalfCheetah problem in which we impose constraints on the speed of Cheetah in order to force it to run smoothly. As shown in the video, the policy learned by our algorithm results in slower but much smoother movement of Cheetah compared to the policies learned by PPO and Lagrangian⁵ (see Appendix A for the details of the Lagrangian method); (ii) Point-Circle: the agent is rewarded for running in a wide circle, but is constrained to stay within a safe region defined by $|x| \leq x_{\text{lim}}$; (iii) Point-Gather & Ant-Gather: the agent is rewarded for collecting target objects in a terrain map, while being constrained to avoid bombs. The last two tasks were first introduced in [12] by adding constraints to the original MuJoCo tasks *Point* and *Ant* (details are given in Appendix D).

We compare our algorithms with two state-of-the-art unconstrained algorithms: DDPG and PPO, and two constrained methods: Lagrangian with optimized Lagrange multiplier (see Appendix A) and CPO. We use the CPO algorithm that is based on PPO (unlike the original CPO that is based on TRPO) and coincides with our SPPO algorithm derived in Section 4.1. SPPO preserves the essence of CPO by adding the first-order constraint and relative entropy regularization to the policy optimization problem. The main difference between CPO and SPPO is that the latter *does not* perform backtracking line-search in learning rate. We compare with SPPO instead of CPO to 1) avoid the additional computational complexity of line-search in TRPO, while maintaining the performance of PG using PPO, 2) have a back-propagatable version of CPO, and 3) have a fair comparison with other back-propagatable safe PG algorithms, such as our DDPG-based and a -projection algorithms.

Baselines: Figures 1a, 1b, 2a, 2b, 8a, 8b, 9a, 9b show that our Lyapunov-based PG algorithms are stable in learning and all converge to feasible policies with reasonable performance. Figures 1c, 1d, 2c, 2d, 8c, 8d, 9c, 9b show the algorithms in terms of constraint violation during training. These figures indicate that our algorithms quickly stabilize the constraint cost below the threshold, while the unconstrained DDPG and PPO violate the constraints, and Lagrangian tends to jiggle around the threshold. Moreover, it is worth-noting that the Lagrangian method can be sensitive to the initialization of the Lagrange multiplier λ_0 . If λ_0 is too large, it would make policy updates overly conservative, and if it is too small, then we will have more constraint violation. Without further

⁴Videos of MuJoCo experiments can be found in the following link: <https://drive.google.com/file/d/1FwbuEnKN21LWFMKvDCydo2EQVdc1401a/view?usp=sharing>.

⁵Alternatively one might impose constraint on the torque at the Cheetah’s joints to force it to run smoothly, but it is unclear how this constraint can directly control its speed and achieve stability.

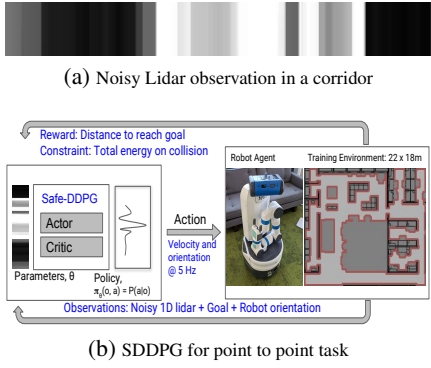


Figure 3: Robot navigation task details.

knowledge about the environment, we treat λ_0 as a hyper-parameter and optimize it via grid-search. More details about the experiments and the results for *Ant-Gather* and *Point-Circle* domains are reported in Appendix D.

a -projection vs. θ -projection: The figures indicate that in many cases DDPG- a and PPO- a converge faster and have lower constraint violation than their θ -projection counterparts (i.e., SDDPG and SPPD). This corroborates with the hypothesis that a -projection is less conservative during policy updates than θ -projection (which is what CPO is based on) and generates smoother gradient updates during end-to-end training.

DDPG vs. PPO: In most experiments (HalfCheetah, PointGather, and AntGather) the DDPG algorithms tend to have faster learning than their PPO counterparts, while the PPO algorithms perform better in terms of constraint satisfaction. The faster learning of DDPG algorithms is due to their improved sample-efficiency resulted from their off-policy nature. However, the covariate-shift⁶ in off-policy data makes constraint satisfaction more challenging for these algorithms.

Safety Constraints: Similar to other state-of-the-art methods, such as CPO and PCPO [26], our proposed model-free Lyapunov-based RL algorithms enforce safety during training without explicit consideration of function approximation error, and thus, have no provable safety guarantee. To prevent constraint violation due to function approximation error, similar to CPO, we offer a safeguard policy update rule that further decreases the constraint cost.

5 Safe Policy Gradient for Robot Navigation

We now evaluate safe policy optimization algorithms on a real robot task – a *map-less* navigation task [7] – where a noisy differential drive robot with limited sensors (Fig. 3a) is required to navigate to a goal outside of its field of view in an unseen environment while avoiding collision. The main objective is to learn a policy that drives the robot to the goal as efficiently as possible, while limiting the impact energy of collisions, since the collision can damage the robot and environment.

The agent’s observations consist of the relative goal position, agent’s velocity, and Lidar measurements (Fig. 3a). The actions are the linear and angular velocity at the robot’s center of the mass.⁷ The transition probability captures the noisy robot’s dynamics, whose exact formulation is unknown to the robot. The robot must navigate to arbitrary goal positions collision-free in a previously unseen environment, without access to the indoor map and any work-space topology. We reward the agent for reaching the goal, which translates to an immediate cost that measures the relative distance to the goal. The cumulative constraint measures the total impact energy of obstacle collisions, with a constraint threshold d_0 that characterizes the agent’s maximum tolerable collision impact energy. Different from the standard approach, where a constraint on collision speed is explicitly imposed to the learning problem at each time step, we emphasize that a CMDP constraint is required here because it allows the robot to lightly brush off the obstacle (such as walls) but prevent it from ramming into any object.

Experimental Results: We evaluate the learning algorithms on success rate and constraint violation averaged over 100 episodes with random initialization. The task is successful if the robot reaches

⁶Here the covariate shift is due to the fact that the training data is generated by a policy different than the one being optimized.

⁷The first dimension is the robot’s desired linear velocity (speed at which the robot should go straight). The second dimension is the robot’s angular velocity - speed at which the robot should turn. Both velocity vectors are applied to the center of mass of the robot.

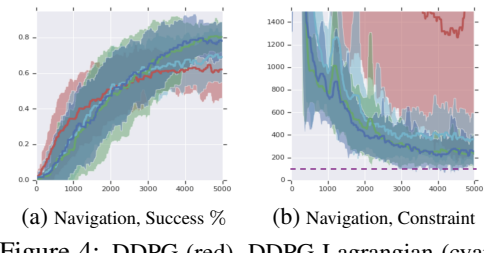


Figure 4: DDPG (red), DDPG-Lagrangian (cyan), SDDPG (blue), SDDPG- a (green) on Robot Navigation. Ours (SDDPG, SDDPG- a) balance between reward and constraint learning. Unit of x-axis is in thousands of steps. The shaded areas represent the 1-SD confidence intervals (over 50 runs). The dashed purple line represents the constraint limit.



Figure 5: Navigation routes for two learned policies in the simulator (left: Lagrangian, middle: SDDPG-*a*), and on-robot experiment of SDDPG-*a* (right).

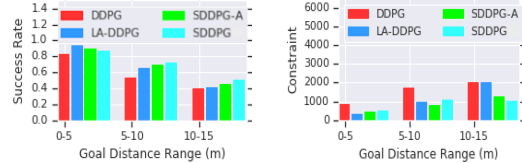


Figure 6: Generalization over success rate (left) and constraint (right) on a different environment, averaged over 100 tasks (random start and goal positions).

the goal before the constraint threshold (total energy of collision) is exhausted. While all methods converge to policies with reasonable performance, Figures 4a and 4b show that the Lyapunov-based PG algorithms have higher success rates, due to their ability to control the balance between constraint violation and minimizing the distance to the goal. Although the unconstrained method often yields a lower distance to the goal, it violates the constraint more frequently leading to a lower success rate. Lagrangian approach is less robust to initialization of parameters, and thus, generally has lower success rate and higher variability than the Lyapunov-based methods. Unfortunately due to function approximation error and stochasticity of the problem, all the algorithms converge pre-maturely with constraint cost above the threshold, possibly due to the overly conservative constraint threshold $d_0 = 100$. Inspection of trajectories shows that the Lagrangian method tends to zigzag and has more collisions, while the SDDPG-*a* chooses a safer path to reach the goal (Fig. 5, left and middle).

Next, we evaluate how well the methods generalize to (i) longer trajectories, and (ii) new environments. We apply each method to train the robot in different tasks in a 22 by 18 meters environment (Fig. 10 in Appendix E), where each task corresponds to the goal placed within 5 to 10 meters from the robot’s initial state. We then test the learned policy in a much larger environment (60 by 47 meters) with goals placed up to 15 meters away from the goal. We observe the success rate of all methods degrades as the goals are further away (Fig. 6). However, both of our safe algorithms outperform unconstrained and Lagrangian methods, while retaining lower constraints in the larger environment (Fig. 6).

Finally, we deployed the SDDPG-*a* policy on the real Fetch robot [27] in an everyday office environment.⁸ Fetch robot weighs 150 kilograms and reaches maximum speed of 7 km/h, making the collision force a safety paramount. Fig. 5 (right) shows the top down view of the robot log. Robot travels through narrow corridors and around people walking through the office for a total of 500 meters to complete five repetitions of 12 tasks, each averages about 10 meters to the goal. The robot robustly avoids both static and dynamic (humans) obstacles coming into its path. We observe additional “wobbling” effects that was not present in simulation. This is likely due to the wheel slippage at the floor that the policy was not trained for. In several occasions when the robot could not find a clear path, the policy instructed the robot to stay put instead of narrowly passing by the obstacle. This is precisely the safety behavior we want to achieve with the Lyapunov-based algorithms.

6 Conclusions and Future Work

We used the notion of Lyapunov functions and developed a class of safe RL algorithms for continuous action problems. Each algorithm in this class is a combination of one of our two proposed projections: θ -projection and a -projection, with any on-policy (e.g., PPO) or off-policy (e.g., DDPG) PG algorithm. We evaluated our algorithms on four high-dimensional simulated robot locomotion MuJoCo tasks and compared them with several baselines. To demonstrate the effectiveness of our algorithms in solving real-world problems, we also applied them to an indoor robot navigation problem, to ensure that the robot’s path is optimal and collision-free. Our results indicate that our algorithms 1) enforce near-safe learning, 2) have better data-efficiency and 3) can be more naturally integrated within the standard end-to-end differentiable PG training pipeline, than the state-of-the-art competitors such as CPO, and finally 4) are scalable to tackle real-world problems. Our work is a step toward developing RL algorithms that can be applied to real-world problems in which enforcing safety constraints is of paramount importance. Future work includes 1) extending a -projection to stochastic policies, 2) deriving theoretically sound and efficient model-free safe RL algorithms, and 3) extensions of the Lyapunov approach to model-based RL and use it for safe exploration.

⁸Videos of Fetch robot navigation can be found in the following link: <https://drive.google.com/file/d/1FwbuEnKN21LWFMKvDCydo2EQVdc14O1a/view?usp=sharing>

References

- [1] V. Mnih, K. Kavukcuoglu, D. Silver, A. Rusu, J. Veness, M. Bellemare, A. Graves, M. Riedmiller, A. Fidjeland, G. Ostrovski, S. Petersen, C. Beattie, A. Sadik, I. Antonoglou, H. King, D. Kumaran, D. Wierstra, S. Legg, and D. Hassabis. Human-level control through deep reinforcement learning. *Nature*, 518(7540):529–533, 2015.
- [2] D. Silver, A. Huang, C. Maddison, A. Guez, L. Sifre, G. van den Driessche, J. Schrittwieser, I. Antonoglou, V. Panneershelvam, M. Lanctot, S. Dieleman, D. Grewe, J. Nham, N. Kalchbrenner, I. Sutskever, T. Lillicrap, M. Leach, K. Kavukcuoglu, T. Graepel, and D. Hassabis. Mastering the game of Go with deep neural networks and tree search. *Nature*, 529(7587):484–489, 2016.
- [3] T. Lillicrap, J. Hunt, A. Pritzel, N. Heess, T. Erez, Y. Tassa, D. Silver, and D. Wierstra. Continuous control with deep reinforcement learning. In *International Conference on Learning Representations*, 2016.
- [4] S. Levine, C. Finn, T. Darrell, and P. Abbeel. End-to-end training of deep visuo-motor policies. *Journal of Machine Learning Research*, 17:1–40, 2016.
- [5] D. Kalashnikov, A. Irpan, P. Sampedro, J. Ibarz, A. Herzog, E. Jang, D. Quillen, E. Holly, M. Kalakrishnan, V. Vanhoucke, and S. Levine. QT-Opt: Scalable deep reinforcement learning for vision-based robotic manipulation. 2018. URL <https://arxiv.org/pdf/1806.10293.pdf>.
- [6] A. Faust, O. Ramirez, M. Fiser, K. Oslund, A. Francis, J. Davidson, and L. Tapia. PRM-RL: Long-range robotic navigation tasks by combining reinforcement learning and sampling-based planning. In *IEEE International Conference on Robot Automation*, pages 5113–5120, 2018.
- [7] H. Chiang, A. Faust, M., and A. Francis. Learning navigation behaviors end-to-end with autorl. *IEEE Robotics and Automation Letters*, 4(2):2007–2014, 2019.
- [8] E. Altman. *Constrained Markov decision processes*, volume 7. CRC Press, 1999.
- [9] E. Altman. Constrained Markov decision processes with total cost criteria: Lagrangian approach and dual linear program. *Mathematical methods of operations research*, 48(3):387–417, 1998.
- [10] P. Geibel and F. Wysotski. Risk-sensitive reinforcement learning applied to control under constraints. *Journal of Artificial Intelligence Research*, 24:81–108, 2005.
- [11] Y. Chow, M. Ghavamzadeh, L. Janson, and M. Pavone. Risk-constrained reinforcement learning with percentile risk criteria. *Journal of Machine Learning Research*, 18(1):6070–6120, 2017.
- [12] J. Achiam, D. Held, A. Tamar, and P. Abbeel. Constrained policy optimization. *arXiv preprint arXiv:1705.10528*, 2017.
- [13] T. Yang, J. Rosca, K. Narasimhan, and P. Ramadge. Projection-based constrained policy optimization. In *ICLR*, 2020.
- [14] J. Schulman, S. Levine, P. Moritz, M. Jordan, and P. Abbeel. Trust region policy optimization. In *Proceedings of the 32nd International Conference on Machine Learning*, pages 1889–1897, 2015.
- [15] Y. Chow, O. Nachum, E. Duenez-Guzman, and M. Ghavamzadeh. A Lyapunov-based approach to safe reinforcement learning. In *Proceedings of Advances in Neural Information Processing Systems 32*, pages 8103–8112, 2018.
- [16] H. Khalil. Nonlinear systems. *Prentice-Hall, New Jersey*, 2(5):5–1, 1996.
- [17] T. Perkins and A. Barto. Lyapunov design for safe reinforcement learning. *Journal of Machine Learning Research*, 3(Dec):803–832, 2002.
- [18] A. Faust, P. Ruymgaart, M. Salman, R. Fierro, and L. Tapia. Continuous action reinforcement learning for control-affine systems with unknown dynamics. *Acta Automatica Sinica Special Issue on Extensions of Reinforcement Learning and Adaptive Control, IEEE/CAA Journal of*, 1(3):323–336, July 2014.

- [19] F. Berkenkamp, M. Turchetta, A. Schoellig, and A. Krause. Safe model-based reinforcement learning with stability guarantees. In *Advances in Neural Information Processing Systems*, pages 908–918, 2017.
- [20] J. Schulman, F. Wolski, P. Dhariwal, A. Radford, and O. Klimov. Proximal policy optimization algorithms. *arXiv preprint arXiv:1707.06347*, 2017.
- [21] G. Dalal, K. Dvijotham, M. Vecerik, T. Hester, C. Paduraru, and Y. Tassa. Safe exploration in continuous action spaces. *arXiv preprint arXiv:1801.08757*, 2018.
- [22] D. Hafner, J. Davidson, and V. Vanhoucke. TensorFlow Agents: Efficient batched reinforcement learning in tensorflow. *arXiv preprint arXiv:1709.02878*, 2017.
- [23] S. Kakade and J. Langford. Approximately optimal approximate reinforcement learning. In *ICML*, volume 2, pages 267–274, 2002.
- [24] B. Amos and Z. Kolter. Optnet: Differentiable optimization as a layer in neural networks. *arXiv preprint arXiv:1703.00443*, 2017.
- [25] E. Todorov, T. Erez, and Y. Tassa. Mujoco: A physics engine for model-based control. In *Intelligent Robots and Systems (IROS), 2012 IEEE/RSJ International Conference on*, pages 5026–5033. IEEE, 2012.
- [26] T. Yang, J. Rosca, K. Narasimhan, and P. Ramadge. Projection-based constrained policy optimization. In *International Conference on Learning Representations*, 2019.
- [27] M. Wise, M. Ferguson, D. King, E. Diehr, and D. Dymesich. Fetch & Freight: Standard platforms for service robot applications. In *Workshop on Autonomous Mobile Service Robots held at the 2016 International Joint Conference on Artificial Intelligence*, 2016.
- [28] D. Bertsekas. *Nonlinear programming*. Athena scientific Belmont, 1999.
- [29] R. Sutton, D. McAllester, S. Singh, and Y. Mansour. Policy gradient methods for reinforcement learning with function approximation. In *Proceedings of Advances in Neural Information Processing Systems 12*, pages 1057–1063, 2000.
- [30] V. Mnih, K. Kavukcuoglu, D. Silver, A. Graves, I. Antonoglou, D. Wierstra, and M. Riedmiller. Playing Atari with deep reinforcement learning. *arXiv preprint arXiv:1312.5602*, 2013.
- [31] D. Bertsekas. *Dynamic programming and optimal control*, volume 1-2. Athena scientific Belmont, MA, 2005.
- [32] T. Schaul, J. Quan, I. Antonoglou, and D. Silver. Prioritized experience replay. *arXiv preprint arXiv:1511.05952*, 2015.
- [33] J. Schulman, P. Moritz, S. Levine, M. Jordan, and P. Abbeel. High-dimensional continuous control using generalized advantage estimation. *arXiv preprint arXiv:1506.02438*, 2015.

A The Lagrangian Approach to Safe RL

A.1 Lagrangian Method

Lagrangian method is a straightforward way to address the constraint $\mathcal{D}_{\pi_\theta}(x_0) \leq d_0$ in CMDPs. Lagrangian method adds the constraint costs $d(x)$ to the task costs $c(x, a)$ and transform constrained optimization to a penalty form, i.e., $\min_{\theta \in \Theta} \max_{\lambda \geq 0} \mathbb{E}[\sum_{t=0}^{\infty} c(x_t, a_t) + \lambda d(x_t) | \pi_\theta, x_0] - \lambda d_0$. The method then jointly optimizes θ and λ to find a saddle-point of the penalized objective. The optimization of θ may be performed by any PG algorithm on the augmented cost $c(x, a) + \lambda d(x)$, while λ is optimized by stochastic gradient descent. Although the Lagrangian approach is easy to implement, in practice, it often violates the constraints during training. While at each step during training, the objective encourages finding a safe solution, the current value of λ may lead to an unsafe policy. This is why the Lagrangian method may not be suitable for solving problems in which safety is crucial during training.

We first state a number of mild technical and notational assumptions that we make throughout this section.

Assumption 1 (Differentiability). *For any state-action pair (x, a) , $\pi_\theta(a|x)$ is continuously differentiable in θ and $\nabla_\theta \pi_\theta(a|x)$ is a Lipschitz function in θ for every $x \in \mathcal{X}$ and $a \in \mathcal{A}$.*

Assumption 2 (Strict Feasibility). *There exists a transient policy $\pi_\theta(\cdot|x)$ such that $\mathcal{D}_{\pi_\theta}(x_0) < d_0$ in the constrained problem.*

Assumption 3 (Step Sizes). *The step size schedules $\{\alpha_{3,k}\}$, $\{\alpha_{2,k}\}$, and $\{\alpha_{1,k}\}$ satisfy*

$$\sum_k \alpha_{1,k} = \sum_k \alpha_{2,k} = \sum_k \alpha_{3,k} = \infty, \quad (8)$$

$$\sum_k \alpha_{1,k}^2, \quad \sum_k \alpha_{2,k}^2, \quad \sum_k \alpha_{3,k}^2 < \infty, \quad (9)$$

$$\alpha_{1,k} = o(\alpha_{2,k}), \quad \alpha_{2,k} = o(\alpha_{3,k}). \quad (10)$$

Assumption 1 imposes smoothness on the optimal policy. Assumption 2 guarantees the existence of a local saddle point in the Lagrangian analysis. Assumption 3 refers to step sizes corresponding to policy updates and indicates that the update corresponding to $\{\alpha_{3,k}\}$ is on the fastest time-scale, the update corresponding to $\{\alpha_{2,k}\}$ is on the intermediate time-scale, and the update corresponding to $\{\alpha_{1,k}\}$ is on the slowest time-scale. As this assumption refers to user-defined parameters, they can always be chosen to be satisfied.

To solve the CMDP, we employ the Lagrangian relaxation procedure [28] to convert it to the following unconstrained problem:

$$\max_{\lambda \geq 0} \min_{\theta} \left(L(\theta, \lambda) \triangleq \mathcal{C}_{\pi_\theta}(x_0) + \lambda (\mathcal{D}_{\pi_\theta}(x_0) - d_0) \right), \quad (11)$$

where λ is the Lagrange multiplier. Notice that $L(\theta, \lambda)$ is a linear function in λ . Then, there exists a local saddle point (θ^*, λ^*) for the minimax optimization problem $\max_{\lambda \geq 0} \min_{\theta} L(\theta, \lambda)$, such that for some $r > 0$, $\forall \theta \in \mathbb{R}^\kappa \cap B_{\theta^*}(r)$, and $\forall \lambda \in [0, \lambda_{\max}]$, we have

$$L(\theta, \lambda^*) \geq L(\theta^*, \lambda^*) \geq L(\theta^*, \lambda), \quad (12)$$

where $B_{\theta^*}(r)$ is a hyper-dimensional ball centered at θ^* with radius $r > 0$.

In the following, we present a policy gradient (PG) algorithm and an actor-critic (AC) algorithm. While the PG algorithm updates its parameters after observing several trajectories, the AC algorithm is incremental and updates its parameters at each time-step.

We now present a policy gradient algorithm to solve the optimization problem (11). The idea of the algorithm is to descend in θ and ascend in λ using the gradients of $L(\theta, \lambda)$ w.r.t. θ and λ , i.e.,

$$\nabla_\theta L(\theta, \lambda) = \nabla_\theta (\mathcal{C}_{\pi_\theta}(x_0) + \lambda \mathcal{D}_{\pi_\theta}(x_0)), \quad \nabla_\lambda L(\theta, \lambda) = \mathcal{D}_{\pi_\theta}(x_0) - d_0. \quad (13)$$

The unit of observation in this algorithm is a system trajectory generated by following the current policy π_{θ_k} . At each iteration, the algorithm generates N trajectories by following the current policy π_{θ_k} , uses them to estimate the gradients in (13), and then uses these estimates to update the parameters θ, λ . Let $\xi = \{x_0, a_0, c_0, x_1, a_1, c_1, \dots, x_{T-1}, a_{T-1}, c_{T-1}, x_T\}$ be a trajectory generated by following the policy θ , where $x_T = x_{\text{Tar}}$ is the target state of the system and T is the (random) stopping

time. The cost, constraint cost, and probability of ξ are defined as $\mathcal{C}(\xi) = \sum_{k=0}^{T-1} \gamma^k c(x_k, a_k)$, $\mathcal{D}(\xi) = \sum_{k=0}^{T-1} \gamma^k d(x_k)$, and $\mathbb{P}_\theta(\xi) = P_0(x_0) \prod_{k=0}^{T-1} \pi_\theta(a_k|x_k) P(x_{k+1}|x_k, a_k)$, respectively. Based on the definition of $\mathbb{P}_\theta(\xi)$, one obtains $\nabla_\theta \log \mathbb{P}_\theta(\xi) = \sum_{k=0}^{T-1} \nabla_\theta \log \pi_\theta(a_k|x_k)$.

Algorithm 1 Lagrangian Trajectory-based Policy Gradient Algorithm

Input: parameterized policy $\pi(\cdot|\cdot; \theta)$
Initialization: policy parameter $\theta = \theta_0$, and the Lagrangian parameter $\lambda = \lambda_0$
for $i = 0, 1, 2, \dots$ **do**
 for $j = 1, 2, \dots$ **do**
 Generate N trajectories $\{\xi_{j,i}\}_{j=1}^N$ by starting at x_0 and following the policy θ_i .
 end for
 θ **Update:** $\theta_{i+1} = \theta_i - \alpha_{2,i} \frac{1}{N} \sum_{j=1}^N \nabla_\theta \log \mathbb{P}_\theta(\xi_{j,i})|_{\theta=\theta_i} (\mathcal{C}(\xi_{j,i}) + \lambda_i \mathcal{D}(\xi_{j,i}))$
 λ **Update:** $\lambda_{i+1} = \Gamma_\Lambda \left[\lambda_i + \alpha_{1,i} \left(-d_0 + \frac{1}{N} \sum_{j=1}^N \mathcal{D}(\xi_{j,i}) \right) \right]$
 end for

Algorithm 1 contains the pseudo-code of our proposed PG algorithm. What appears inside the parentheses on the right-hand-side of the update equations are the estimates of the gradients of $L(\theta, \lambda)$ w.r.t. θ, λ (estimates of the expressions in (13)). Gradient estimates of the Lagrangian function are given by

$$\nabla_\theta L(\theta, \lambda) = \sum_{\xi} \mathbb{P}_\theta(\xi) \cdot \nabla_\theta \log \mathbb{P}_\theta(\xi) (\mathcal{C}_{\pi_\theta}(\xi) + \lambda \mathcal{D}_{\pi_\theta}(\xi)), \quad \nabla_\lambda L(\theta, \lambda) = -d_0 + \sum_{\xi} \mathbb{P}_\theta(\xi) \cdot \mathcal{D}(\xi),$$

where the likelihood gradient is

$$\begin{aligned} \nabla_\theta \log \mathbb{P}_\theta(\xi) &= \nabla_\theta \left\{ \sum_{k=0}^{T-1} \log P(x_{k+1}|x_k, a_k) + \log \pi_\theta(a_k|x_k) + \log \mathbf{1}\{x_0 = x^0\} \right\} \\ &= \sum_{k=0}^{T-1} \nabla_\theta \log \pi_\theta(a_k|x_k) = \sum_{k=0}^{T-1} \frac{1}{\pi_\theta(a_k|x_k)} \nabla_\theta \pi_\theta(a_k|x_k). \end{aligned}$$

In Algorithm 1, Γ_Λ is a projection operator to $[0, \lambda_{\max}]$, i.e., $\Gamma_\Lambda(\lambda) = \arg \min_{\hat{\lambda} \in [0, \lambda_{\max}]} \|\lambda - \hat{\lambda}\|_2^2$, which ensures the convergence of the algorithm. Recall from Assumption 3 that the step-size schedules satisfy the standard conditions for stochastic approximation algorithms, and ensure that the policy parameter θ update is on the fast time-scale $\{\alpha_{2,i}\}$, and the Lagrange multiplier λ update is on the slow time-scale $\{\alpha_{1,i}\}$. This results in a two time-scale stochastic approximation algorithm that has been shown to converge to a (local) saddle point of the objective function $L(\theta, \lambda)$. This convergence proof makes use of standard results in stochastic approximation theory, because in the limit when the step-size is sufficiently small, analyzing the convergence of PG is equivalent to analyzing the stability of an ordinary differential equation (ODE) w.r.t. its equilibrium point.

In PG, the unit of observation is a system trajectory. This may result in high variance for the gradient estimates, especially when the length of the trajectories is long. To address this issue, we propose two actor-critic algorithms that use value function approximation in the gradient estimates and update the parameters incrementally (after each state-action transition). We present two actor-critic algorithms for optimizing (11). These algorithms are still based on the above gradient estimates. Algorithm 2 contains the pseudo-code of these algorithms. The projection operator Γ_Λ is necessary to ensure the convergence of the algorithms. Recall from Assumption 3 that the step-size schedules satisfy the standard conditions for stochastic approximation algorithms, and ensure that the critic update is on the fastest time-scale $\{\alpha_{3,k}\}$, the policy update $\{\alpha_{2,k}\}$ is on the intermediate timescale, and finally the Lagrange multiplier update is on the slowest time-scale $\{\alpha_{1,k}\}$. This results in three time-scale stochastic approximation algorithms.

Using the PG theorem from [29], one can show that

$$\nabla_\theta L(\theta, \lambda) = \nabla_\theta V_\theta(x_0) = \frac{1}{1-\gamma} \sum_{x,a} \mu_\theta(x, a|x_0) \nabla \log \pi_\theta(a|x) Q_\theta(x, a), \quad (20)$$

Algorithm 2 Lagrangian Actor-Critic Algorithm

Input: Parameterized policy $\pi(\cdot| \cdot; \theta)$ and value function feature vector $\phi(\cdot)$
Initialization: policy parameters $\theta = \theta_0$; Lagrangian parameter $\lambda = \lambda_0$; value function weight $v = v_0$
while TRUE **do**

for $k = 0, 1, 2, \dots$ **do**

Sample $a_k \sim \pi(\cdot|x_k; \theta_k)$; $c_{\lambda_k}(x_k, a_k) = c(x_k, a_k) + \lambda_k d(x_k)$; $x_{k+1} \sim P(\cdot|x_k, a_k)$;

// AC Algorithm:

TD Error: $\delta_k(v_k) = c_{\lambda_k}(x_k, a_k) + \gamma \hat{V}_{\phi_k}(x_{k+1}) - \hat{V}_{\phi_k}(x_k)$ (14)

Critic Update: $v_{k+1} = v_k + \zeta_3(k)\delta_k(v_k)\psi(x_k)$ (15)

θ Update: $\theta_{k+1} = \theta_k - \zeta_2(k)\nabla_{\theta} \log \pi_{\theta}(a_k|x_k) \cdot \delta_k(v_k)/1 - \gamma$ (16)

λ Update: $\lambda_{k+1} = \Gamma_{\Lambda} \left(\lambda_k + \zeta_1(k)(-d_0 + \frac{1}{N} \sum_{j=1}^N \mathcal{D}(\xi_{j,i})) \right)$ (17)

// NAC Algorithm:

Critic Update: $w_{k+1} = \left(I - \zeta_3(k)\nabla_{\theta} \log \pi_{\theta}(a_k|x_k)|_{\theta=\theta_k} (\nabla_{\theta} \log \pi_{\theta}(a_k|x_k)|_{\theta=\theta_k})^\top \right) w_k + \zeta_3(k)\delta_k(v_k)\nabla_{\theta} \log \pi_{\theta}(a_k|x_k)|_{\theta=\theta_k}$ (18)

θ Update: $\theta_{k+1} = \theta_k - \zeta_2(k)w_k/1 - \gamma$ (19)

Other Updates: Follow from Eqs. 14, 15, and 17.

end for

end while

where μ_{θ} is the discounted visiting distribution and Q_{θ} is the action-value function of policy θ . We can show that $\frac{1}{1-\gamma}\nabla \log \pi_{\theta}(a_k|x_k) \cdot \delta_k$ is an unbiased estimate of $\nabla_{\theta} L(\theta, \lambda)$, where

$$\delta_k = c_{\lambda}(x_k, a_k) + \gamma \hat{V}_{\theta}(x_{k+1}) - \hat{V}_{\theta}(x_k)$$

is the temporal-difference (TD) error, and \hat{V}_{θ} is an estimator of the value function V_{θ} .

Traditionally, for convergence guarantees in actor-critic algorithms, the critic uses linear approximation for the value function $V_{\theta}(x) \approx v^{\top} \psi(x) = \hat{V}_{\theta,v}(x)$, where the feature vector $\psi(\cdot)$ belongs to a low-dimensional space \mathbb{R}^{κ_2} . The linear approximation $\hat{V}_{\theta,v}$ belongs to a low-dimensional subspace $S_V = \{\Psi v | v \in \mathbb{R}^{\kappa_2}\}$, where Ψ is a short-hand notation for the set of features, i.e., $\Psi(x) = \psi^{\top}(x)$. Recently with the advances in deep neural networks, it has become increasingly popular to model the critic with a deep neural network, based on the objective function of minimizing the MSE of Bellman residual w.r.t. \hat{V}_{θ} or Q_{θ} [30].

B The Lyapunov Approach to Solve CMDPs

In this section, we revisit the *Lyapunov approach* to solving CMDPs that was proposed by [15] and report the mathematical results that are important in developing our safe policy optimization algorithms. To start, without loss of generality, we assume that we have access to a *baseline* feasible policy of (1), π_B ; i.e., π_B satisfies $\mathcal{D}_{\pi_B}(x_0) \leq d_0$. We define a set of Lyapunov functions w.r.t. initial state $x_0 \in \mathcal{X}$ and constraint threshold d_0 as

$$\mathcal{L}_{\pi_B}(x_0, d_0) = \{L : \mathcal{X} \rightarrow \mathbb{R}_{\geq 0} : T_{\pi_B, d}[L](x) \leq L(x), \forall x \in \mathcal{X}; L(x_0) \leq d_0\},$$

and call the constraints in this feasibility set the *Lyapunov constraints*. For any arbitrary Lyapunov function $L \in \mathcal{L}_{\pi_B}(x_0, d_0)$, we denote by

$$\mathcal{F}_L(x) = \{\pi(\cdot|x) \in \Delta : T_{\pi, d}[L](x) \leq L(x)\},$$

the set of L -induced Markov stationary policies. Since $T_{\pi, d}$ is a contraction mapping [31], any L -induced policy π has the property $\mathcal{D}_\pi(x) = \lim_{k \rightarrow \infty} T_{\pi, d}^k[L](x) \leq L(x), \forall x \in \mathcal{X}$. Together with the property that $L(x_0) \leq d_0$, they imply that any L -induced policy is a feasible policy of (1). However, in general, the set $\mathcal{F}_L(x)$ does not necessarily contain an optimal policy of (1), and thus, it is necessary to design a Lyapunov function (w.r.t. a baseline policy π_B) that provides this guarantee. In other words, the main goal is to construct a Lyapunov function $L \in \mathcal{L}_{\pi_B}(x_0, d_0)$ such that

$$L(x) \geq T_{\pi^*, d}[L](x), \quad L(x_0) \leq d_0. \quad (21)$$

Chow et al. [15] show in their Theorem 1 that 1) without loss of optimality, the Lyapunov function can be expressed as

$$L_\epsilon(x) := \mathbb{E} \left[\sum_{t=0}^{\infty} \gamma^t (d(x_t) + \epsilon(x_t)) \mid \pi_B, x \right],$$

where $\epsilon(x) \geq 0$ is some auxiliary constraint cost uniformly upper-bounded by

$$\epsilon^*(x) := 2D_{\max} D_{TV}(\pi^* || \pi_B)(x) / (1 - \gamma),$$

and 2) if the baseline policy π_B satisfies the condition

$$\max_{x \in \mathcal{X}} \epsilon^*(x) \leq D_{\max} \cdot \min \left\{ (1 - \gamma) \frac{d_0 - \mathcal{D}_{\pi_B}(x_0)}{D_{\max}}, \frac{D_{\max} - (1 - \gamma)\bar{\mathcal{D}}}{D_{\max} + (1 - \gamma)\bar{\mathcal{D}}} \right\},$$

where $\bar{\mathcal{D}} = \max_{x \in \mathcal{X}} \max_{\pi} \mathcal{D}_\pi(x)$ is the maximum constraint cost, then the Lyapunov function candidate L_{ϵ^*} also satisfies the properties of (21), and thus, its induced feasible policy set $\mathcal{F}_{L_{\epsilon^*}}$ contains an optimal policy. Furthermore, suppose that the distance between the baseline and optimal policies can be estimated efficiently. Using the set of L_{ϵ^*} -induced feasible policies and noting that the *safe* Bellman operator $T[V](x) = \min_{\pi \in \mathcal{F}_{L_{\epsilon^*}}(x)} T_{\pi, c}[V](x)$ is monotonic and contractive, one can show that $T[V](x) = V(x), \forall x \in \mathcal{X}$, has a unique fixed point V^* , such that $V^*(x_0)$ is a solution of (1) and an optimal policy can be constructed via greedification, i.e., $\pi^*(\cdot|x) \in \arg \min_{\pi \in \mathcal{F}_{L_{\epsilon^*}}(x)} T_{\pi, c}[V^*](x)$. This shows that under the above assumption, (1) can be solved using standard dynamic programming (DP) algorithms. While this result connects CMDP with Bellman's principle of optimality, verifying whether π_B satisfies this assumption is challenging when a good estimate of $D_{TV}(\pi^* || \pi_B)$ is not available. To address this issue, Chow et al. [15] propose to approximate ϵ^* with an auxiliary constraint cost $\tilde{\epsilon}$, which is the *largest* auxiliary cost satisfying the Lyapunov condition $L_{\tilde{\epsilon}}(x) \geq T_{\pi_B, d}[L_{\tilde{\epsilon}}](x), \forall x \in \mathcal{X}$, and the safety condition $L_{\tilde{\epsilon}}(x_0) \leq d_0$. The intuition here is that the larger $\tilde{\epsilon}$, the larger the set of policies $\mathcal{F}_{L_{\tilde{\epsilon}}}$. Thus, by choosing the largest such auxiliary cost, we hope to have a better chance of including the optimal policy π^* in the set of feasible policies. Specifically, $\tilde{\epsilon}$ is computed by solving the following linear program (LP):

$$\tilde{\epsilon} \in \arg \max_{\epsilon: \mathcal{X} \rightarrow \mathbb{R}_{\geq 0}} \left\{ \sum_{x \in \mathcal{X}} \epsilon(x) : d_0 - \mathcal{D}_{\pi_B}(x_0) \geq \mathbf{1}(x_0)^\top \left(I - \gamma \left\{ P(x'|x, \pi_B(x)) \right\}_{x, x' \in \mathcal{X}} \right)^{-1} \epsilon \right\}, \quad (22)$$

where $\mathbf{1}(x_0)$ represents a one-hot vector in which the non-zero element is located at $x = x_0$. When π_B is a feasible policy, this problem has a non-empty solution. Furthermore, according to the derivations in [15], the maximizer of (22) has the following form:

$$\tilde{\epsilon}(x) = \frac{(d_0 - \mathcal{D}_{\pi_B}(x_0)) \cdot \mathbf{1}\{x = \underline{x}\}}{\mathbb{E} \left[\sum_{t=0}^{\infty} \gamma^t \mathbf{1}\{x_t = \underline{x}\} \mid x_0, \pi_B \right]} \geq 0,$$

Algorithm 3 Safe Policy Iteration (SPI)

Input: Initial feasible policy π_0 ;
for $k = 0, 1, 2, \dots$ **do**
 Step 0: With $\pi_b = \pi_k$, evaluate the Lyapunov function L_{ϵ_k} , where ϵ_k is a solution of (22)
 Step 1: Evaluate the cost value function $V_{\pi_k}(x) = \mathcal{C}_{\pi_k}(x)$; Then update the policy by solving the following problem: $\pi_{k+1}(\cdot|x) \in \operatorname{argmin}_{\pi \in \mathcal{F}_{L_{\epsilon_k}}(x)} T_{\pi,c}[V_{\pi_k}](x), \forall x \in \mathcal{X}$
end for
Return Final policy π_{k^*}

where $\underline{x} \in \arg \min_{x \in \mathcal{X}} \mathbb{E} \left[\sum_{t=0}^{\infty} \gamma^t \mathbf{1}\{x_t = x\} \mid x_0, \pi_B \right]$. They also show that by further restricting $\tilde{\epsilon}(x)$ to be a constant function, the maximizer is given by

$$\tilde{\epsilon}(x) = (1 - \gamma) \cdot (d_0 - \mathcal{D}_{\pi_B}(x_0)), \quad \forall x \in \mathcal{X}.$$

Using the construction of the Lyapunov function $L_{\tilde{\epsilon}}$, [15] propose the safe policy iteration (SPI) algorithm (see Algorithm 3) in which the Lyapunov function is updated via *bootstrapping*, i.e., at each iteration $L_{\tilde{\epsilon}}$ is recomputed using (22) w.r.t. the current baseline policy. At each iteration k , this algorithm has the following properties: **1) Consistent Feasibility**, i.e., if the current policy π_k is feasible, then π_{k+1} is also feasible; **2) Monotonic Policy Improvement**, i.e., $\mathcal{C}_{\pi_{k+1}}(x) \leq \mathcal{C}_{\pi_k}(x)$ for any $x \in \mathcal{X}$; and **3) Asymptotic Convergence**. Despite all these nice properties, SPI is still a value-function-based algorithm, and thus, it is not straightforward to use it in continuous action problems. The main reason is that the greedification step becomes an optimization problem over the continuous set of actions that is not necessarily easy to solve. In Section 3, we show how we use SPI and its nice properties to develop safe policy optimization algorithms that can handle continuous action problems. Our algorithms can be thought as combinations of DDPG or PPO (or any other on-policy or off-policy policy optimization algorithm) with a SPI-inspired critic that evaluates the policy and computes its corresponding Lyapunov function. The computed Lyapunov function is then used to guarantee safe policy update, i.e., the new policy is selected from a restricted set of safe policies defined by the Lyapunov function of the current policy.

C Technical Details of the Safe Policy Gradient Algorithms

In this section, we first provide the details of the derivation of the θ -projection and a -projection procedures described in Section 3, and then provide the pseudo-codes of our safe PG algorithms.

C.1 Derivation of θ -projection in Lyapunov-based Safe PG

To derive our θ -projection algorithms, we first consider the original Lyapunov constraint in (3) that is given by

$$\int_{a \in \mathcal{A}} (\pi_\theta(a|x) - \pi_B(a|x)) Q_{L_{\pi_B}}(x, a) da \leq \tilde{\epsilon}(x), \quad \forall x \in \mathcal{X},$$

where the baseline policy is parameterized as $\pi_B = \pi_{\theta_B}$. Using the first-order Taylor series expansion w.r.t. $\theta = \theta_B$, at any arbitrary $x \in \mathcal{X}$, the term $\mathbb{E}_{a \sim \pi_\theta} [Q_{L_{\theta_B}}(x, a)] = \int_{a \in \mathcal{A}} \pi_\theta(a|x) Q_{L_{\pi_B}}(x, a) da$ on left-hand-side of the above inequality can be written as

$$\mathbb{E}_{a \sim \pi_\theta} [Q_{L_{\theta_B}}(x, a)] = \mathbb{E}_{a \sim \pi_{\theta_B}} [Q_{L_{\theta_B}}(x, a)] + \left\langle (\theta - \theta_B), \nabla_\theta \mathbb{E}_{a \sim \pi_\theta} [Q_{L_{\theta_B}}(x, a)] |_{\theta=\theta_B} \right\rangle + O(\|\theta - \theta_B\|^2),$$

which implies that

$$\int_{a \in \mathcal{A}} (\pi_\theta(a|x) - \pi_B(a|x)) Q_{L_{\pi_B}}(x, a) da = \left\langle (\theta - \theta_B), \nabla_\theta \mathbb{E}_{a \sim \pi_\theta} [Q_{L_{\theta_B}}(x, a)] |_{\theta=\theta_B} \right\rangle + O(\|\theta - \theta_B\|^2).$$

Note that the objective function of the constrained minimization problem in (4) contains a regularization term: $\frac{\beta}{2} \left\langle (\theta - \theta_B), \nabla_\theta^2 \overline{D}_{\text{KL}}(\theta, \theta_B) |_{\theta=\theta_B} (\theta - \theta_B) \right\rangle$ that controls the distance $\|\theta - \theta_B\|$ to be small. For most practical purposes, here one can assume the higher-order term $O(\|\theta - \theta_B\|^2)$ to be much smaller than the first-order term $\left\langle (\theta - \theta_B), \nabla_\theta \mathbb{E}_{a \sim \pi_\theta} [Q_{L_{\theta_B}}(x, a)] |_{\theta=\theta_B} \right\rangle$. Therefore, one can approximate the original Lyapunov constraint in (3) with the following constraint:

$$\left\langle (\theta - \theta_B), \nabla_\theta \mathbb{E}_{a \sim \pi_\theta} [Q_{L_{\theta_B}}(x, a)] |_{\theta=\theta_B} \right\rangle \leq \tilde{\epsilon}(x), \quad \forall x \in \mathcal{X}.$$

Furthermore, following the same line of arguments used in TRPO (to transform the max D_{KL} constraint to an average \overline{D}_{KL} constraint, see Eq. 12 in [14]), a more numerically stable way is to *approximate* the Lyapunov constraint using the average constraint surrogate, i.e.,

$$\left\langle (\theta - \theta_B), \frac{1}{M} \sum_{i=1}^M \nabla_\theta \mathbb{E}_{a \sim \pi_\theta} [Q_{L_{\theta_B}}(x_i, a)] |_{\theta=\theta_B} \right\rangle \leq \frac{1}{M} \sum_{i=1}^M \tilde{\epsilon}(x_i).$$

Now consider the special case when auxiliary constraint surrogate is chosen as a constant, i.e., $\tilde{\epsilon} = (1 - \gamma)(d_0 - \mathcal{D}_{\pi_{\theta_B}}(x_0))$. The justification of such choice comes from analyzing the solution of optimization problem (22). Then, one can write the Lyapunov action-value function $Q_{L_{\theta_B}}(x, a)$ as

$$Q_{L_{\theta_B}}(x, a) = \mathbb{E} \left[\sum_{t=0}^{\infty} \gamma^t d(x_t) | \pi_B, x_0 = x, a_0 = a \right] + \frac{\tilde{\epsilon}}{1 - \gamma}.$$

Since the second term is independent of θ , for any state $x \in \mathcal{X}$, the gradient term $\nabla_\theta \mathbb{E}_{a \sim \pi_\theta} [Q_{L_{\theta_B}}(x, a)]$ can be simplified as

$$\nabla_\theta \mathbb{E}_{a \sim \pi_\theta} [Q_{L_{\theta_B}}(x, a)] = \int_a \pi_\theta(a|x) \nabla_\theta \log \pi_\theta(a|x) Q_{W_{\theta_B}}(x, a) da = \nabla_\theta \mathbb{E}_{a \sim \pi_\theta} [Q_{W_{\theta_B}}(x, a)],$$

where $W_{\theta_B}(x) = T_{\pi_B, d}[W_{\theta_B}](x)$ and $Q_{W_{\theta_B}}(x, a) = d(x) + \gamma \sum_{x'} P(x'|x, a) W_{\theta_B}(x')$ are the constraint value function and constraint state-action value function, respectively. The second equality is based on the standard log-likelihood gradient property in PG algorithms [29].

Collectively, one can then re-write the Lyapunov average constraint surrogate as

$$\left\langle (\theta - \theta_B), \frac{1}{M} \sum_{i=1}^M \nabla_\theta \mathbb{E}_{a \sim \pi_\theta} [Q_{W_{\theta_B}}(x_i, a)] |_{\theta=\theta_B} \right\rangle \leq \tilde{\epsilon},$$

where $\tilde{\epsilon}$ is the auxiliary constraint cost defined specifically by the Lyapunov-based approach, to guarantee constraint satisfaction. By expanding the auxiliary constraint cost $\tilde{\epsilon}$ on the right-hand-side, the above constraint is equivalent to the constraint used in CPO, i.e.,

$$\mathcal{D}_{\pi_{\theta_B}}(x_0) + \frac{1}{1-\gamma} \langle (\theta - \theta_B), \frac{1}{M} \sum_{i=1}^M \nabla_\theta \mathbb{E}_{a \sim \pi_\theta} [Q_{W_{\theta_B}}(x_i, a)] |_{\theta=\theta_B} \rangle \leq d_0.$$

C.2 Derivations of a -projection in Lyapunov-based Safe PG

For any arbitrary state $x \in \mathcal{X}$, consider the following constraint in the safety-layer projection problem given in (6):

$$Q_{L_{\pi_B}}(x, a) - Q_{L_{\pi_B}}(x, \pi_B(x)) \leq \tilde{\epsilon}(x).$$

Using first-order Taylor series expansion of the Lyapunov state-action value function $Q_{L_{\pi_B}}(x, a)$ w.r.t. action $a = \pi_B(x)$, the Lyapunov value function $Q_{L_{\pi_B}}(x, a)$ can be re-written as

$$Q_{L_{\pi_B}}(x, a) = Q_{L_{\pi_B}}(x, \pi_B(x)) + (a - \pi_B(x))^\top g_{L_{\pi_B}}(x) + O(\|a - \pi_B(x)\|^2).$$

Note that the objective function of the action-projection problem in (7) contains a regularization term $\frac{\eta(x)}{2} \|a - \pi_B(x)\|^2$ that controls the distance $\|a - \pi_B(x)\|$ to be small. For most practical purposes, here one can assume the higher-order term $O(\|a - \pi_B(x)\|^2)$ to be much smaller than the first-order term $(a - \pi_B(x))^\top g_{L_{\pi_B}}(x)$. Therefore, one can approximate the original action-based Lyapunov constraint in (6) with the constraint $(a - \pi_B(x))^\top g_{L_{\pi_B}}(x) \leq \tilde{\epsilon}(x)$ that is the constraint in (7). Similar to the analysis of the θ -projection approach, if the auxiliary cost $\tilde{\epsilon}$ is state-independent, the action-gradient term $g_{L_{\pi_B}}(x)$ is equal to the gradient of the constraint action-value function $\nabla_a Q_{W_{\theta_B}}(x, a)|_{a=\pi_B(x)}$, where $Q_{W_{\theta_B}}$ is the state-action constraint value function w.r.t. the baseline policy. The rest of the proof follows the results from Proposition 1 in [21]. This completes the derivations of the a -projection approach.

C.3 Pseudo-codes of Our Safe PG Algorithms

Algorithms 4 and 5 contain the pseudo-code of our safe Lyapunov-based policy gradient (PG) algorithms with θ -projection and a -projection, respectively.

C.4 Practical Implementation of Our Safe PG Algorithms

Due to function approximation errors, even with the Lyapunov constraints, in practice a safe PG algorithm may take a bad step and produce an infeasible policy update and cannot automatically recover from such a bad step. To address this issue, similar to [12], we propose the following *safeguard* policy update rule to decrease the constraint cost: $\theta_{k+1} = \theta_k - \alpha_{sg,k} \nabla_\theta \mathcal{D}_{\pi_\theta}(x_0)|_{\theta=\theta_k}$, where $\alpha_{sg,k}$ is the learning rate for the safeguard update. If $\alpha_{sg,k} >> \alpha_k$ (learning rate of PG), then with the safeguard update, θ will quickly recover from the bad step, however, it might be overly conservative. This approach is principled because as soon as π_{θ_k} is unsafe/infeasible w.r.t. the CMDP constraints, the algorithm uses a limiting search direction. One can directly extend this safeguard update to the multiple-constraint scenario by doing gradient descent over the constraint that has the worst violation.

Another remedy to reduce the chance of constraint violation is to do *constraint tightening* on the constraint cost threshold. Specifically, instead of d_0 , one may pose the constraint based on $d_0 \cdot (1 - \delta)$, where $\delta \in (0, 1)$ is the factor of safety for providing additional buffer to constraint violation. Additional techniques in cost-shaping have been proposed in [12] to smooth out the sparse constraint costs. While these techniques can further ensure safety, construction of the cost-shaping term requires knowledge of the environment, which makes the safe PG algorithms more complicated.

Algorithm 4 Lyapunov-based Safe PG with θ -projection (SDDPG and SPPO)

Input: Initial feasible policy π_0 ;

for $k = 0, 1, 2, \dots$ **do**

Step 0: Generate N trajectories $\{\xi_{j,k}\}_{j=1}^N$ that start at x_0 and follow policy $\pi_b = \pi_{\theta_k}$ for T steps

Step 1: Using trajectories $\{\xi_{j,k}\}_{j=1}^N$, estimate critic $Q_\theta(x, a)$ and constraint critic $Q_{D,\theta}(x, a)$:

- For DDPG, these functions are trained by minimizing the MSE of the Bellman residual, and we may use off-policy samples from the replay buffer [32];
- For PPO, these functions are estimated by the generalized advantage function technique from [33]

Step 2: Based on the closed-form solution of a QP problem with a LP constraint in Section 10.2 of [12], calculate λ_k^* by the following formula:

$$\lambda_k^* = \left[\frac{-\beta_k \bar{\epsilon} - (\nabla_\theta Q_\theta(\bar{x}, \bar{a}) |_{\theta=\theta_k})^\top H(\theta_k)^{-1} \nabla_\theta Q_{D,\theta}(\bar{x}, \bar{a}) |_{\theta=\theta_k}}{(\nabla_\theta Q_{D,\theta}(\bar{x}, \bar{a}) |_{\theta=\theta_k})^\top H(\theta_k)^{-1} \nabla_\theta Q_{D,\theta}(\bar{x}, \bar{a}) |_{\theta=\theta_k}} \right]_+,$$

where

$$\nabla_\theta Q_\theta(\bar{x}, \bar{a}) = \frac{1}{N} \sum_{x,a \in \xi_{j,k}, 1 \leq j \leq N} \sum_{t=0}^{T-1} \gamma^t \nabla_\theta \log \pi_\theta(a|x) Q_\theta(x, a),$$

$$\nabla_\theta Q_{D,\theta}(\bar{x}, \bar{a}) = \frac{1}{N} \sum_{x,a \in \xi_{j,k}, 1 \leq j \leq N} \sum_{t=0}^{T-1} \gamma^t \nabla_\theta \log \pi_\theta(a|x) Q_{D,\theta}(x, a),$$

β_k is the adaptive penalty weight of the $\overline{D}_{\text{KL}}(\pi || \pi_{\theta_k})$ regularizer, and $H(\theta_k) = \nabla_\theta^2 \overline{D}_{\text{KL}}(\pi || \pi_\theta) |_{\theta=\theta_k}$ is the Hessian of this term

Step 3: Update the policy parameter using the gradient of the objective function;

 For DDPG

$$\theta_{k+1} \leftarrow \theta_k - \alpha_k \cdot \frac{1}{NT} \sum_{x \in \xi_{j,k}, 1 \leq j \leq N} \nabla_\theta \pi_\theta(x) |_{\theta=\theta_k} \cdot (\nabla_a Q_{\theta_k}(x, a) + \lambda_k^* \nabla_a Q_{D,\theta_k}(x, a)) |_{a=\pi_{\theta_k}(x)}$$

 For PPO

$$\theta_{k+1} \leftarrow \theta_k - \frac{\alpha_k}{N\beta_k} H(\theta_k)^{-1} \sum_{x_{j,t}, a_{j,t} \in \xi_{j,k}, 1 \leq j \leq N} \sum_{t=0}^{T-1} \gamma^t \nabla_\theta \log \pi_\theta(a_{j,t}|x_{j,t}) |_{\theta=\theta_k} (Q_{\theta_k}(x_{j,t}, a_{j,t}) + \lambda_k^* Q_{D,\theta_k}(x_{j,t}, a_{j,t}))$$

Step 4: For all $x \in \mathcal{X}$, compute the feasible action probability $a^*(x)$ via action projection in the safety layer that takes inputs $\nabla_a Q_L(x, a) = \nabla_a Q_{D,\theta_k}(x, a)$, $\forall a \in \mathcal{A}$ and $\epsilon(x) = (1-\gamma)(d_0 - Q_{D,\theta_k}(x_0, \pi_k(x_0)))$

end for

Return Final policy π_{θ_k*}

Algorithm 5 Lyapunov-based Safe PG with a -projection (SDDPG- a and SPPO- a)

Input: Initial feasible policy π_0 ;

for $k = 0, 1, 2, \dots$ **do**

Step 0: Generate N trajectories $\{\xi_{j,k}\}_{j=1}^N$ that start at x_0 and follow policy $\pi_b = \pi_{\theta_k}$ for T steps

Step 1: Using trajectories $\{\xi_{j,k}\}_{j=1}^N$, estimate critic $Q_\theta(x, a)$ and constraint critic $Q_{D,\theta}(x, a)$:

- For DDPG, these functions are trained by minimizing the MSE of the Bellman residual, and we may use off-policy samples from the replay buffer [32];
- For PPO, these functions are estimated by the generalized advantage function technique from [33]

Step 2: Update the policy parameter using the gradient of the objective function;

$$\text{For DDPG} \quad \theta_{k+1} \leftarrow \theta_k - \alpha_k \cdot \frac{1}{NT} \sum_{x \in \xi_{j,k}, 1 \leq j \leq N} \nabla_\theta \pi_\theta(x) |_{\theta=\theta_k} \cdot \nabla_a Q_{\theta_k}(x, a) |_{a=\pi_{\theta_k}(x)};$$

$$\text{For PPO} \quad \theta_{k+1} \leftarrow \theta_k - \frac{\alpha_k}{N\beta_k} H(\theta_k)^{-1} \sum_{x_{j,t}, a_{j,t} \in \xi_{j,k}, 1 \leq j \leq N} \sum_{t=0}^{T-1} \gamma^t \nabla_\theta \log \pi_\theta(a_{j,t}|x_{j,t}) |_{\theta=\theta_k} Q_{\theta_k}(x_{j,t}, a_{j,t})$$

 where β_k is the adaptive penalty weight of the $\overline{D}_{\text{KL}}(\pi || \pi_{\theta_k})$ regularizer, and $H(\theta_k) = \nabla_\theta^2 \overline{D}_{\text{KL}}(\pi || \pi_\theta) |_{\theta=\theta_k}$ is the Hessian of this term

Step 3: For all $x \in \mathcal{X}$, compute the feasible action probability $a^*(x)$ via action projection in the safety layer that takes inputs $\nabla_a Q_L(x, a) = \nabla_a Q_{D,\theta_k}(x, a)$, $\forall a \in \mathcal{A}$ and $\epsilon(x) = (1-\gamma)(d_0 - Q_{D,\theta_k}(x_0, \pi_k(x_0)))$

end for

Return Final policy π_{θ_k*}

D Experimental Setup in MuJoCo Tasks

Our experiments are performed on safety-augmented versions of standard MuJoCo domains [25].

HalfCheetah-Safe. The agent is a the standard HalfCheetah (a 2-legged simulated robot rewarded for running at high speed) augmented with safety constraints. We choose the safety constraints to be defined on the speed limit. We constrain the speed to be less than 1, i.e., constraint cost is thus $1[|v| > 1]$. Episodes are of length 200. The constraint threshold is 50.

Point Circle. This environment is taken from [12]. The agent is a point mass (controlled via a pivot). The agent is initialized at $(0, 0)$ and rewarded for moving counter-clockwise along a circle of radius 15 according to the reward $\frac{-dx \cdot y + dy \cdot x}{1 + |\sqrt{x^2 + y^2} - 15|}$, for position x, y and velocity dx, dy . The safety constraint is defined as the agent staying in a position satisfying $|x| \leq 2.5$. The constraint cost is thus $1[|x| > 2.5]$. Episodes are of length 65. The constraint threshold is 7.

Point Gather. This environment is taken from [12]. The agent is a point mass (controlled via a pivot) and the environment includes randomly positioned apples (2 apples) and bombs (8 bombs). The agent given a reward of 10 for each apple collected and a penalty of -10 for each bomb. The safety constraint is defined as the number of bombs collected during the episode. Episodes are of length 15. The constraint threshold is 4 for DDPG and 2 for PPO.

Ant Gather. This environment is the same as Point Circle, only with an Ant agent (quadrupedal simulated robot). Each episode is initialized with 8 apples and 8 bombs. The agent receives a reward of 10 for each apple collected, a penalty of -20 for each bomb collected, and a penalty of -20 if the episode terminates prematurely (because the Ant falls). Episodes are of length at most 500. The constraint threshold is 10 and 5 for DDPG and PPO, respectively.

Figure 7 shows the visualization of the above domains used in our experiments.

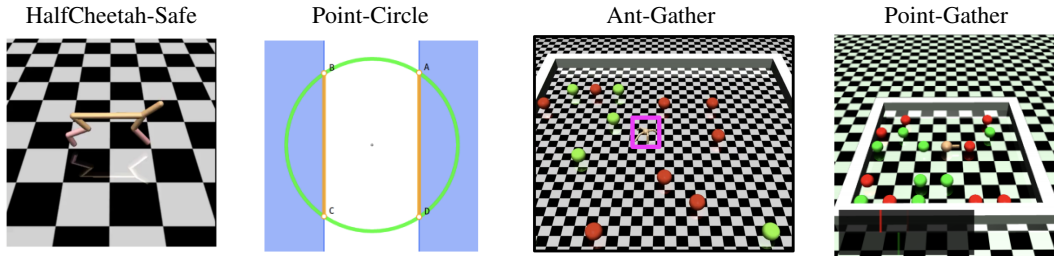


Figure 7: The Robot Locomotion Control Tasks

In these experiments, there are three different agents: (1) a point-mass ($\mathcal{X} \subseteq \mathbb{R}^9, A \subseteq \mathbb{R}^2$); an ant quadruped robot ($\mathcal{X} \subseteq \mathbb{R}^{32}, A \subseteq \mathbb{R}^8$); and (3) a half-cheetah ($\mathcal{X} \subseteq \mathbb{R}^{18}, A \subseteq \mathbb{R}^6$). For all experiments, we use two neural networks with two hidden layers of size $(100, 50)$ and ReLU activation to model the mean and log-variance of the Gaussian actor policy, and two neural networks with two hidden layers of size $(200, 50)$ and tanh activation to model the critic and constraint critic. To build a low variance sample gradient estimate, we use GAE- λ [33] to estimate the advantage and constraint advantage functions, with a hyper-parameter $\lambda \in (0, 1)$ optimized by grid-search.

On top of GAE- λ , in all experiments and for each algorithm (SDDPG, SPPO, SDDPG- a , SPPO- a , CPO, Lagrangian, and the unconstrained PG counterparts), we systematically explored different parameter settings by doing grid-search over the following factors: (i) learning rates in the actor-critic algorithm, (ii) batch size, (iii) regularization parameters of the policy relative entropy term, (iv) with-or-without natural policy gradient updates, (v) with-or-without the emergency safeguard PG updates (see Appendix C.4 for more details). Although each algorithm might have a different parameter setting that leads to the optimal performance in training, the results reported here are the best ones for each algorithm, chosen by the same criteria (which is based on the value of return plus certain degree of constraint satisfaction). To account for the variability during training, in each learning curve, a 1-SD confidence interval is also computed over 10 separate random runs (under the same parameter setting).

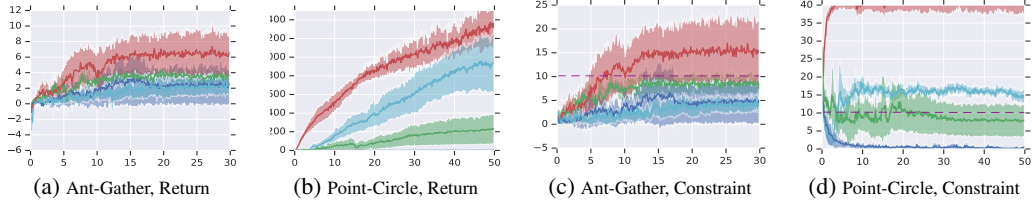


Figure 8: DDPG (red), DDPG-Lagrangian (cyan), SDDPG (blue), SDDPG-a (green) on Ant-Gather and Point-Circle. Ours SDDPG and SDDPG-a algorithms perform stable and safe learning, although the dynamics and cost functions are unknown, control actions are continuous, and deep function approximation is used. Unit of x-axis is in thousands of episodes. Shaded areas represent the 1-SD confidence intervals (over 10 random seeds). The dashed purple line in the two right figures represents the constraint limit.

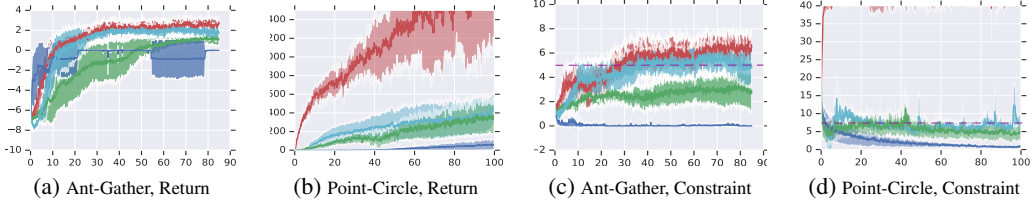


Figure 9: PPO (red), PPO-Lagrangian (cyan), SPPO (blue), SPPO-a (green) on Ant-Gather and Point-Circle. SPPO-a performs stable and safe learning, when the dynamics and cost functions are unknown, control actions are continuous, and deep function approximation is used.

D.1 More Explanations on MuJoCo Results

In all numerical experiments and for each algorithm (SPPO, SDDPG, SPPO-a, SDDPG-a, CPO, Lagrangian, and the unconstrained PG counterparts), we systematically explored various hyper-parameter settings by doing grid-search over the following factors: (i) learning rates in the actor-critic algorithm, (ii) batch size, (iii) regularization parameters of the policy relative entropy term, (iv) with-or-without natural policy gradient updates, (v) with-or-without the emergency safeguard PG updates (see Appendix C.4 for more details). Although each algorithm might have a different parameter setting that leads to the optimal training performance, the results reported in the paper are the best ones for each algorithm, chosen by the same criteria (which is based on value of return + certain degree of constraint satisfaction).

In our experiments, we compare the two classes of safe RL algorithms, one derived from θ -projection (constrained policy optimization) and one from the a -projection (safety layer), with the unconstrained and Lagrangian baselines in four problems: PointGather, AntGather, PointCircle, and HalfCheetah-Safe. We perform these experiments with both off-policy (DDPG) and on-policy (PPO) versions of the algorithms.

In PointCircle DDPG, although the Lagrangian algorithm significantly outperforms the safe RL algorithms in terms of return, it violates the constraint more often. The only experiment in which Lagrangian performs similarly to the safe algorithms in terms of both return and constraint violation is PointCircle PPO. In all other experiments that are performed in the HalfCheetahSafe, PointGather and AntGather domains, either (i) the policy learned by Lagrangian has a significantly lower performance than that learned by one of the safe algorithms (see HalfCheetahSafe DDPG, PointGather DDPG, AntGather DDPG), or (ii) the Lagrangian method violates the constraint during training, while the safe algorithms do not (see HalfCheetahSafe PPO, PointGather PPO, AntGather PPO). This clearly illustrates the effectiveness of our Lyapunov-based safe RL algorithms, when compared to Lagrangian method.

E Experimental Setup in the Robot Navigation Problem

Mapless navigation task is a continuous control task with a goal of navigating a robot to any arbitrary goal position collision-free and without memory of the workspace topology. The goal is usually within 5 – 10 meters from the robot agent, but it is not visible to the agent before the task starts, due to both limited sensor range and the presence of obstacles that block a clear line of sight. The agent’s observations, $\mathbf{x} = (\mathbf{g}, \dot{\mathbf{g}}, \mathbf{l}) \in \mathbb{R}^{68}$, consists of the relative goal position, the relative goal velocity, and the Lidar measurements. Relative goal position, \mathbf{g} , is the relative polar coordinates between the goal position and the current robot pose, and $\dot{\mathbf{g}}$ is the time derivative of \mathbf{g} , which indicates the speed of the robot navigating to the goal. This information is available from the robot’s localization sensors. Vector \mathbf{l} is the noisy Lidar input (Fig. 3a), which measures the nearest obstacle in a direction within a 220° field of view split in 64 bins, up to 5 meters in depth. The action is given by $\mathbf{a} \in \mathbb{R}^2$, which is linear and angular velocity vector at the robot’s center of the mass. The transition probability $P : \mathcal{X} \times \mathcal{A} \rightarrow \mathcal{X}$ captures the noisy differential drive robot dynamics. Without knowing the full non-linear system dynamics, we here assume knowledge of a simplified blackbox kinematics simulator operating at 5Hz in which Gaussian noise, $\mathcal{N}(0, 0.1)$, is added to both the observations and actions in order to model the noise in sensing, dynamics, and action actuators in real-world. The objective of the P2P task is to navigate the robot to reach within 30 centimeters from any real-time goal. While the dynamics of this system is simpler than that of HalfCheetah. But unlike the MuJoCo tasks where the underlying dynamics are deterministic, in this robot experiment the sensor, localization, and dynamics noise paired with partial world observations and unexpected obstacles make this safe RL much more challenging. More descriptions about the indoor robot navigation problem and its implementation details can be found in Section 3 and 4 of [7]. Fetch robot weights 150 kilograms, and reaches maximum speed of 7 km/h making the collision force a safety paramount.

Here the CMDP is non-discounting and has a finite-horizon of $T = 100$. We reward the agent for reaching the goal, which translates to an immediate cost of $c(\mathbf{x}, \mathbf{a}) = \|\mathbf{g}\|^2$, which measures the relative distance to goal. To measure the impact energy of obstacle collisions, we impose an immediate constraint cost of $d(\mathbf{x}, \mathbf{a}) = \|\dot{\mathbf{g}}\| \cdot \mathbf{1}\{\|\mathbf{l}\| \leq r_{\text{impact}}\}/T$, where r_{impact} is the impact radius w.r.t. the Lidar depth signal, to account for the speed during collision, with a constraint threshold d_0 that characterizes the agent’s maximum tolerable collision impact energy to any objects. (Here the total impact energy is proportional to the robot’s speed during any collisions.) Under this CMDP framework (Fig. 3b), the main goal is to train a policy π^* that drives the robot along the shortest path to the goal and to limit the average impact energy of obstacle collisions. Furthermore, due to limited data any intermediate point-to-point policy is deployed on the robot to collect more samples for further training, therefore guaranteeing safety during training is critical in this application.

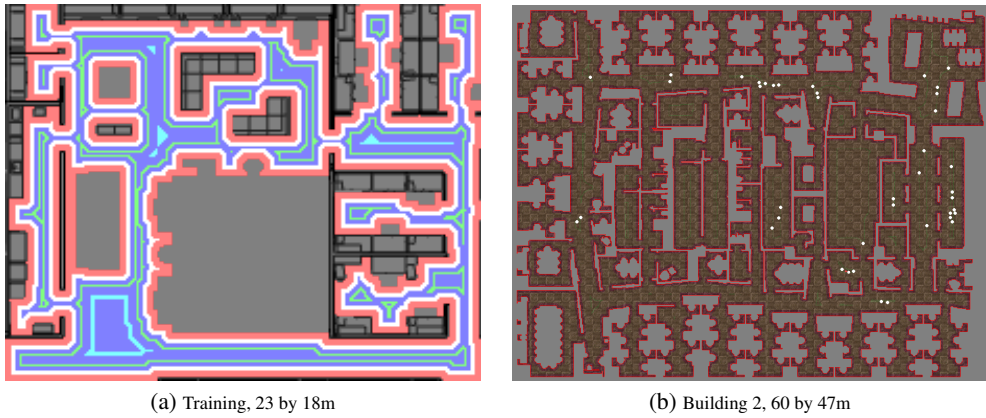


Figure 10: (a) Training and (b) evaluation environments, generated from real office building plans. The evaluation environment is an order of magnitude bigger.